

# Buncefield: Reconciliation of Evidence with Mechanisms of Blast

James Venart  
University of New Brunswick  
Fredericton, NB, Canada

## 1 Introduction

Seldom do accidental large-scale explosions provide sufficiently accurate forensic data to enable unambiguous conclusions as to blast mechanism(s). However the enormous explosion at the UK Buncefield fuel storage depot at about 6am 11 December 2005, we think, is an exception. This explosion resulted in much damage to the surrounding area with large fires, involving 23 fuel/oil storage tanks that persisted for many days. A vast amount of data in the form of site measurements and observations, witness statements, photographs and CCTV footage was studied, catalogued and analysed [1]. The area covered by the vapour cloud was estimated to be around 120,000m<sup>2</sup> with the average height of the cloud being about 2 to 3m. This gives a volume of between 240,000 and 360,000m<sup>3</sup>. Evidence cited in [1] suggested the emergency pump house as one source of ignition.

The two most commonly known explosion mechanisms are deflagration and detonation. Both possibilities were assessed by the Buncefield Major Incident Investigation Board (MIIB) for their consistency with the observed explosion characteristics [1]. Deflagration was found to be inconsistent with the significant near field damage to most objects and cars. Detonation, however, was inconsistent with damage suffered by buildings within the flammable cloud. CFD modelling of the area immediately surrounding the emergency pump house (PH) supported a suggestion that congestion of trees and undergrowth along Cherry Trees Lane and Buncefield Lane could have allowed flame acceleration to several hundred m/s. Such high velocity may have provided an opportunity for transition from deflagration to detonation, DDT, and thus the progression of a single detonation front, from this source, into the vapour cloud from the Pump House Lagoon (PHL) W and to the S-W; see also [2] and [3].

The characteristics for direct initiation to detonation vs. DDT may be found in [4]; “[t]he former mode is dependent upon an ignition source driving a blast wave of sufficient strength such that the igniter is directly responsible for initiating the detonation. The latter case begins with a deflagration initiated by some relatively weak energy source which accelerates, through interactions with its surroundings, into a coupled shock wave-reaction zone structure characteristic of a detonation: Puttock [5] refers this to as a “Bang Box” ignition. Direct initiation by a concentrated source requires an extremely large energy deposition relative to such a deflagrative ignition.”

In this paper we very briefly review our past work on this accident [6, 7]. Based upon this we conclude that the statement made in [1], and by others, that “*the most likely scenario ...was a deflagration outside the emergency pump house that changed into a detonation due to flame acceleration in the undergrowth and trees along Three Cherry Trees Lane*” is incorrect.

## 2 What Needs Explanation

In order to clarify this statement one must explain:

- the vapour cloud dispersion
- the ignition processes
- the development and progression of the explosion(s)
- vehicle damage and movement
- storage tank damage
- building damage
- lamp post behavior, and
- the CCTV records

Figure 1 is a photograph of the site. North is to the top of the photograph. There are superimposed labels indicating major buildings; vehicle groups and car parks; CCTV camera locations, their lines of sight; as well as the area of vegetative scorching: indicative of the extent of the vapour cloud. Three Cherry Trees Lane is at the top of the photograph and Buncefield Lane runs N to S just W of the bund enclosing three large storage tanks; the centre one, T912, being the tank which overflowed for nearly 40 minutes allowing over 300 tonnes of winter-grade gasoline at 15 °C to escape, vaporize and mix with air to form the vapour cloud. The resulting cloud overtopped the surrounding bund and dispersed. At no time was the cloud, beyond the bund walls, above the upper flammable limit (UFL). Atmospheric conditions at the time were: no wind, stable conditions, 0°C, 99% relative humidity [8].

### 2.1 Dispersion Model

A NIST FDS5 CFD model was constructed for the western half of the Buncefield site [7]. FDS5 uses what is called an LES turbulence model [9]. The area modelled encompassed the car parks, the Northgate (NG), Fuji (F), RO and 3-Com buildings. The model comprised nearly two million cells ranging in size from 0.5 x 2 x 2m to 2 x 2 x 2m, at height, split by a mirror boundary along the N-S centreline of the line of tanks that included, in the centre, the one that overflowed. Fence lines and vegetation (trees and shrubs) were included using a version of FDS developed for use in wildland-urban fire interfaces [10]. A Schmidt Number of 1.7 and a Prandtl Number of 0.79 was taken as representative values based upon the determined properties [11] of the overflowing dispersing fuel-air cloud [12].

Figure 2 illustrates the dispersion modelling result for the lower flammable limit (LFL) boundary at about 2400s. The LFL boundary of the simulation is seen to conform very closely to the observed regions of vegetative scorching in the western areas between the NG and Fuji and 3-Com buildings illustrated by the cloud's extent; Figure 1. Temporal and geometric comparisons with the CCTV record were reasonable [7].

### 2.2 Ignition

There were in fact several potential sources of ignition. First there was confirmed an enclosed and then vented explosion from within the pump-house (PH) into the pump-house lagoon (PHL) [1]. This, if contained, would have resulted in the ignition of approximately one to two tonnes of hydrocarbon in a fuel-air mixture at -3°C (as determined from the dispersion model). This material would have been contained within the space formed by the tree-lined

intersections of Three Cherry Trees Lane, Buncefield Lane and the northern bund wall to the area of overflow. This deflagration is postulated to have immediately formed a fireball [6]. This then would have lifted off and its combustion “whoosh” would have resulted in a significant pressure wave and following wind. These would have traversed the carparks to the S and W of the PHL. The strength of this was sufficient to move, momentarily, a chair and papers S along the E face of the RO building as determined from CCTV records [6].

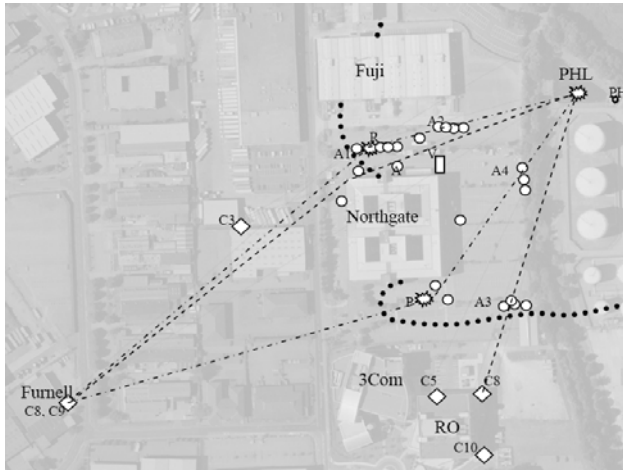


Figure 1. Buncefield site plan indicating building, camera and vehicle locations; Cameras  $\diamond$ , Vehicles  $\circ$ , Cloud extent  $\bullet\bullet\bullet\bullet$  [6].

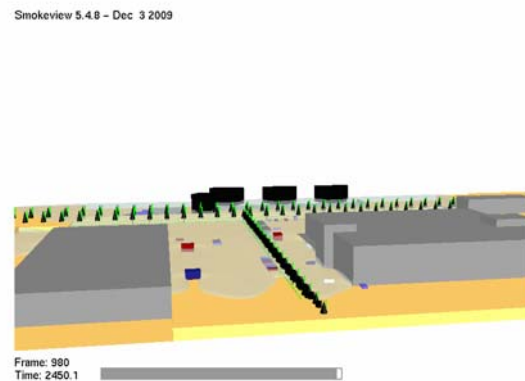


Figure 2. The NIST FDS5 LFL dispersion model of the Buncefield release at ~2400s. View E between the NG and Fuji buildings from the western edge of the computational domain [7].

The pressure wave's following wind would have resulted in disturbances – mixing and turbulence – within the cold, stratified, and previously dispersed vapour cloud; especially along its lean western extremities; between the Northgate and Fuji, and Northgate and 3-Com buildings and could have activated vehicle anti-theft and remote keyless entry (RKE) alarms of affected vehicles. Ignitions there could then have resulted in closed and then vented deflagrations into the now turbulent fuel-air cloud causing local DDTs [6].

### 2.3 Explosion; development and progression

The detonations resulting would not necessarily have been simultaneous – but in fact nearly so – by the order of 100's of ms or so. These would have jetted E from the affected locations (R and P, Figure 1) back towards the PHL and the Buncefield Lane perimeter boundary, crushing and displacing vehicles [6]. The large residue of uncombusted fuel/air mixture now left against the East face of the NG building could now ignite and result in a very large sooty deflagration against the east wall of the NG building. The time taken for all these steps would have been of the order of two to three seconds as indicated from the CCTV record [6].

### 2.4 Vehicles

Many vehicles located in the car parks within the vapour cloud were crushed, moved, and had debaded and deflated tires after the explosion. Haider et al [13] had determined that for normally inflated tires, side wall pressures of at least 0.8MPa are required to debad and deflate them.

Some vehicles had also changed position in the car parks during the explosion. In particular vehicle groups A1 to A4 (Figure 1) had been shifted East and a simple model to estimate this

had been developed [6]. The size of vehicles considered, side-on or lengthwise, means that the positive phase blast wave transits the object over about 2ms, an appreciable portion of the assumed 5.4ms positive detonative blast duration [1].

The analyses assumed the maximum positive phase peak blast pressure as 1.8MPa since comparison to corresponding vehicle damage inflicted by condensed phase explosive experiments [1] on back calculation, and assuming an ideal, or true, shock front, used a maximum reflected side-on pressure of 5MPa: a value similar to that for a maximum dynamic pressure of 3.2MPa. 1.8MPa is also the CJ (Chapman-Jouget) detonation pressure for Butane; a major component of the fuel. Corresponding positive phase dynamic pressures on the vehicle could now be evaluated based upon an assumed linear variation of blast pressure with loading time.

The governing differential equation for a vehicle of mass  $m$  subject to an air drag force  $F_d$  and sliding friction force  $F_f$  were solved and the results for two vehicle types are given in Table 1. The positive pressure load step was followed by a negative one over a period 160ms based upon analyses outlined in [1]. Following these two load steps there was a period of free sliding until the vehicle came to rest. The breaking of vehicle windows and the tearing of frangible panels, and thus the reduction of blast wind affected areas, was considered to take place in 2 and 3ms for a car and van respectively [14]. After these time periods drag affected areas were reduced.

Two different vehicle types were simulated: (a) a van of 2000kg and initial area of 4m<sup>2</sup> and reduced end on flow area, due to blast damage, of 2m<sup>2</sup>; and (b) a car of 1300kg mass with initial side area of 5m<sup>2</sup> and reduced flow area of 4m<sup>2</sup>; the reductions due to crushing, loss of windows and frangible panels. For the range of Reynolds and Mach Numbers under consideration  $C_D$  was considered to be of the order of 1 [15].

Vehicle	Duration (s)	Velocity (m/s)	Distance (m)
Van	0.68	13.4	2.5
Car	0.32	25.0	1.8

Table 1. Summary of vehicle sliding, duration, peak velocity, and displacement [6].

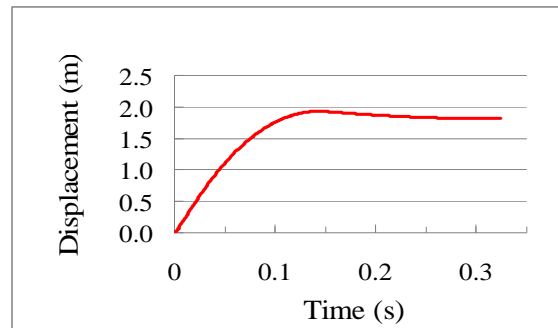


Figure 3. Car displacement for a 5ms positive detonation blast [6].

Figure 3 illustrates the car displacement where it can be clearly seen that the positive phase impulse dominates vehicle motion. Due to the consistency and intensity of vehicle damage over such large and open areas it must be concluded that these aspects of the ‘explosion’ were indeed detonative.

### 2.5 Storage Tanks

There were several empty, or partially filled, tanks within the tank farm that were damaged in a characteristic fashion – T910 (Bund A); T911, T914 (Bund B); and T6. These failures consisted of the vessels being uniformly circumferentially crushed about mid-height (relative to fill level) into several lobes with plastic wrinkles; the roofs blown off – partially or

completely (T910); and the roof rafters still, for the most part, attached to the outer tank circumference and exposed. For these tanks (~25m diameter) the number of lobes was between 18 and 20. For smaller tanks, for example, T601 to T603; the transfer storage tanks (6m diameter and 9.8m high), the deformations, though still crushing with lobes and wrinkles, these were more numerous and complex; though these too had their roofs torn off. Apparent reductions in volume ranged from between 55 to 60 percent for T601 and T910 respectively. This type of deformation is characteristic of what is called elastic dynamic pulse buckling and results from a suddenly applied uniform radial impulse [16]. Figure 4 is the aerial overview of the tank arrangements within the bunds taken from the W.

Simple analysis [7] concluded that tanks T910 and T601 were crushed by elastic impulse pulse buckling with average blast loading overpressures of between 0.38 and 0.85MPa.

### 2.6 Buildings

Detailed ground truth assessment of the blast damage to the Fuji and Northgate buildings suggested that they had only been subjected overpressures in the range of 23 to 27kPa (FEM analyses of the reinforced panels on the E face of the NG building [1]). The observation made was that *“the damage observed to the panels on the Northgate building must have been caused by loading consistent with a large scale deflagration...without significant high-order detonation effects.”*

### 2.7 Lamp Posts

Reference [6], in their analyses of CCTV records from the RO and Furnel Buildings noted that the Buncefield event was very complex consisting of two major deflagrative and two, near simultaneous, detonative events. Reference [1] and others, however, concluded that the explosion resulted from flame acceleration up Three Cherry Tree Lane to DDT and then W into the Fuji and NG car parks and down Buncefield Lane; i.e., a continuously developing event. Directional evidence in the form the deformation and snapping off of lampposts, fence posts, CCTV masts, trees, etc. and *assumed* representative of the negative phase pressure loading was used in support of this conclusion. There were, however, several inconsistencies in the observed data for the lampposts. In particular most lampposts in the car park E of the NG Building appeared to be vertical and not deformed – though many had been abraded by dust and grit on particular sides at their bases. This observation, based upon the assumption that the abrasion was the result of a negative pressure phase of the explosion, was used to infer blast direction. On the other hand lampposts, fence posts, and other indicators (e.g. trees) at the S edge of the Fuji car park were badly deformed, bent and some collapsed or snapped/fractured most pointing E or NE – some confusingly so. For example Figure 5 shows a fractured lamppost felled to the NE (with another to the W behind it felled to the E). Here the perimeter fence between the Fuji car park and Buncefield Lane appears blown overtop of the already felled lamppost. In an attempt to understand this and other behaviour, several lamppost FE (Finite Element) models were constructed and subjected to blast loadings using the ideal blast model taken from [6]. Lamp posts subjected to such loadings were snapped off by the applied positive phase of the blast in much the same way as seen in the figure [7].

### 2.8 CCTV Records

There were several groups of CCTV security cameras located both on and off site beyond the extent of the vapour cloud at Buncefield. Details regarding their placement and view are given in Figure 1. These records provided information on illumination as well as camera motion and

debris behavior induced by wind and blast. Frame by frame analyses were made in [1] and in greater detail in [5]. In summary Reference [6] indicates a record of deflagrative/explosive events lasting from 2500 to 3000ms from formation, of what might be termed a PHL fire-ball, to the commencement of the strong negative pressure phase of the explosion(s) and deflagrations. Strong negative phase developments (i.e. windows being sucked out of buildings) are not recorded by any of the cameras until after about 2500ms.



Figure 4: Aerial view to East of Bund A and its tanks. Tank T912 is in the centre foreground, T910, which was empty at the time of the incident, is to the right of T912; T601 to T603 are at the top of the photograph. [1].



Figure 5: Fuji carpark lampposts: Lamppost in foreground has been hit by blast, snapped and then felled NE. The Fuji carpark Buncefield perimeter fence has next been blown down, up over the felled lamppost base, and then dragged over the fallen pole. A similar pole in the background has also been snapped and blown down to the E.

### 3 DISCUSSION

Since Buncefield there have been at least two further large vapour cloud explosions; the Gulf Oil refinery in Puerto Rico (October 23, 2009) and the Indian Oil Company's (IOC) refinery in Jaipur, India (October 29, 2009). In Buncefield's case "it was concluded that the overpressure within the cloud was generally greater than 200kPa." This actually is an understatement by a factor of about 10 based upon the observed vehicle, lamppost, and storage tank damage.

Furthermore there should be no debate relative to whether or not there were detonations rather than fast deflagrations. The severity of the carpark vehicle damage and the tank and lamppost behavior clearly indicates detonations. Furthermore only a detonation could have traversed the over 100m of unobstructed space E from the car P with its flame/shock structure intact; the flame front for a fast deflagration would have faltered and rapidly reverted to normal flame speeds over such a distance.

The lack of detonation damage to the Fuji, NG, and 3-Com Buildings (pressure damages assessed at between 23 to 27kPa) also clearly suggests that any detonative wave fronts must have passed W to E *between* these structures and then *into* the tank farm. Blast waves at

angles of incidence normal to the walls of the structures – the NG Building was about 70m to the S of the Fuji Building; the vapour cloud also extended only about 30m S of the NG southern wall – work by [17] indicates reflected overpressure coefficients of only 1 for cases where blast wave angle of incidence are between 80 to 90 degrees even for the highest of incident pressures.

#### 4 CONCLUSION

The considerations above lead to the conclusion that the Buncefield explosion consisted of the following elements;

- A vented explosion within the PH that led to the formation of a deflagrative fireball within the PHL fuel cloud.
- A fireball pressure wave “whoosh” from its lift-off that progressed across the car parks as a solitary wave sensitizing the complete vapour cloud in passage by adiabatic heating and turbulence (wind) as well as moving the chair/papers seen in RO C8.
- The passage of this pressure wave wind, activated several RKE/anti-theft vehicle alarms at the lean, turbulent Western edges of the vapour cloud.
- At least two near simultaneous ignitions, as a result of the alarm activations, caused closed vehicle vented deflagrations/“Bang Box” explosions with local transitions to detonation (DDT) at two locations – the space between the Fuji and NG and the southern NG wall – at the “red” and Porsche vehicles respectively; “R” and “P” in Figure 1.
- These detonation blast waves jetted E into the Fuji and NG car parks, crushing and moving/rotating vehicles and other large objects and then into the tank farm crushing empty or partially filled storage tanks within the bund areas.
- The detonation jets, exiting from the confines formed to the N and S by the NG building, formed recirculation zones within the unburnt fuel against its E face. This resulted in a large deflagration of unconsumed fuel that caused structural and fire damage as well as extensive sooting to the N-E section of the wall noted in the FEM analyses of [1] and its photography.

#### 5 REFERENCES

- [1] Steel Construction Institute (2009). Buncefield Explosion Mechanism; Phase 1, Volumes 1 and 2, HSE, rr718, December, 226 p.
- [2] Bakke, J R, van Wingerden, K, Hoorelbeke, P, Brewerton, R, A study on the effect of trees on gas explosions, Journal of Loss Prevention in the Process Industries (2010). doi:10.1016/j.jlp.2010.08.007.
- [3] Johnson, D M, The potential for vapour cloud explosions; Lessons from the Buncefield accident, Journal of Loss Prevention in the Process Industries (2010). doi:10.1016/j.jlp.2010.06.011.
- [4] Schultz, E, Wintenberger, E, Shepherd, J (1999). Investigation of Deflagration to Detonation Transition for Application to Pulse Detonation Engine Ignition Systems, Proc. 16<sup>th</sup> JANNAF Propulsion Symp., Cocoa Beach, FL, Oct. 8.
- [5] Puttock, J S (1999). Improvements in Guidelines for Prediction of Vapour-Cloud Explosions, OPTP.99.47085R2, Shell Global Solutions, HSE Consultancy, presented Int. Conf. and Workshop on Modeling the Consequences of Accidental Releases of Hazardous Materials, San Francisco, Sept.-Oct.
- [6] Venart, J E S, Rogers, R J (2010 in press). Buncefield: Questions on the Development, Progression, and Severity of the Explosion, Proceedings ISFEH6, Leeds, April.
- [7] Venart, J E S, Rogers, R J (2011 in press). The Buncefield Explosion: Vapour Cloud Dispersion and Other Observations, Proceedings IChemE Hazards XXII, Liverpool, April.
- [8] The Buncefield Incident 11 December 2005: The Final Report of the Major Incident Investigation Board (2008) Vol. 1.

- [9] McGrattan, K, Hostikka, S, Floyd, J, Baum H., Rehm, R, Mell, W, McDermott, R (2009) Fire Dynamics Simulator (FDS) ver. 5, Technical Reference Guide, National Institute of Standards and Technology, Gaithersburg, MD.
- [10] Mell, W., Jenkins, M A, Gould, J, Cheney, P (2007). A physics-based approach to modelling grassland fires, *Int. J. Wildland Fire* **16**: 1–22.
- [11] Huber, M L (1999). NIST Standard Reference Database 4, THERMOPHYSICAL PROPERTIES OF HYDROCARBON MIXTURES, SUPERTRAPP, Ver 3.00, National Institute of Standards and Technology, Gaithersburg, MD.
- [12] Atkinson G., Grant S., Painter D., Shirvill L. & Ungut, A. (2008). Liquid Dispersal and Vapour production During Overfilling Incidents. I Chem E Symp Series No 154.
- [13] Haider, M F, Rogers, R J, Venart, J E S (2010, in press) External pressures required to debeat tyres, Proceedings ISFEH6, Leeds, April.
- [14] Penney, W G (Lord), Samuels, D E J, Scorgie, G C (1970). The Nuclear Explosive Yield at Hiroshima and Nagasaki, *Phil. Trans. R. Soc. Lond.* **A266**: 357-424.
- [15] van Netten, A A & Dewey, J M (1997). A study of blast loading on cantilevers, *Shock Waves* **7**: 175-190.
- [16] Lindberg, H E and Florence, A L (1987). Dynamic Pulse Buckling, Martinus Nijhoff, Dordrecht.
- [17] Rose, T A (2001). PhD Thesis, Cranfield University, An Approach to the Evaluation of Blast Loads on Finite and Semi-Infinite Structures.